

Gate-based quantum annealing without digitization errors

Takuya Hatomura*

*NTT Basic Research Laboratories & NTT Research Center for Theoretical
Quantum Information, NTT Corporation, Kanagawa 243-0198, Japan*

(Dated: October 10, 2024)

Time-dependent Hamiltonian simulation using Trotterization causes two types of errors, i.e., discretization errors and digitization errors. In this paper, we propose a decomposition formula which enables us to completely eliminate digitization errors in digital quantum simulation of quantum annealing. We numerically demonstrate scaling advantage of the present method against the conventional Trotterization approach. We also show that the present method can be applied to quantum annealing with some catalysts. Notably, some combinations of nonstoquastic XX -interaction, bias Z -field, and counterdiabatic Y -field catalysts are included in applications of the present method.

I. INTRODUCTION

Combinatorial optimization is a certain class of mathematical optimization problems [1]. Its applications cover a wide range of topics including practical issues, e.g., transportation [2], logistics [3], finance [4], etc. However, the computational complexity of combinatorial optimization is generally NP-hard [1], which requires an exponential time to be solved exactly. Therefore, it is of utmost importance to develop heuristic algorithms which enable us to obtain good approximate solutions within a polynomial time.

Quantum annealing was proposed as a method of obtaining the ground state or low-energy eigenstates of the Ising spin glass [5]. We try to find the target ground state by adiabatically transforming a Hamiltonian from trivial one whose ground state is known to the target Ising spin glass. Quantum annealing is regarded as a heuristic quantum adiabatic algorithm for combinatorial optimization [6, 7] because many combinatorial optimization problems can be formulated as ground-state search of the Ising spin glass [8]. Performance of quantum annealing depends on adiabaticity of a process. For finding the exact solution or good approximate solutions, a long operation time is required because of the adiabatic condition [9, 10]. In particular, an exponential time is necessary to overcome the first-order transition with an exponentially small energy gap.

Applications of additional fluctuations or biases, which are known as catalyst terms, have been discussed as means of improving quantum annealing [11–14]. In particular, antiferromagnetic XX -interaction terms introduce nonstoquasticity, which causes the sign problem in quantum Monte Carlo simulation, and thus antiferromagnetic XX -interaction terms are regarded as suitable catalysts introducing large quantum fluctuations. Removal of the first-order transitions in infinite-range (mean-field-like) models [11, 12] and improvement of adiabaticity in a locally-interacting model [12] were reported. Introduction of bias Z -field terms was also considered [13, 14].

Appropriate choice of biases improves performance of quantum annealing.

Shortcuts to adiabaticity [15–17] are also candidates for improving quantum annealing. Counterdiabatic driving of shortcuts to adiabaticity introduces additional driving (the counterdiabatic term) which completely cancels out nonadiabatic transitions [18–20]. Thus, the counterdiabatic term could be regarded as a well-designed catalyst. Exact application of counterdiabatic driving to quantum annealing is difficult because theoretical construction requires an exponentially large computational cost and experimental realization requires time-dependent control of many-body and nonlocal interactions. Variational and algebraic approaches enable us to approximately construct local counterdiabatic terms with ansatzes on operator forms [21–24]. A detailed analysis of the counterdiabatic term revealed that Y -field terms and YZ -interaction terms are suitable for local counterdiabatic terms improving quantum annealing [25]. It should be mentioned that a mean-field (classical) analysis of counterdiabatic driving applied to quantum annealing also suggests use of Y -field terms [26, 27].

Quantum annealers which implement quantum annealing with thousands of qubits were already manufactured [28–30]. However, implementation of quantum annealing with catalysts is still challenging. Recently, gate-based quantum processors which enable us to implement universal quantum operations were developed [31–33]. These gate-based quantum processors have potential to implement quantum annealing with catalysts. Indeed, digital realization of adiabatic state preparation [34, 35] and quantum annealing with local counterdiabatic driving (Y -field and YZ -interaction catalysts) [36, 37] has been reported. Moreover, a gate-based algorithm for adiabatic transformation, which was inspired by counterdiabatic driving, was also proposed [38] and its performance was numerically benchmarked [39].

Digitization of time-dependent Hamiltonian dynamics causes discretization and digitization errors [40, 41]. Although intrinsic scaling advantage of digitized adiabatic state preparation [42] and digitized counterdiabatic driving [43, 44] was pointed out, large number of time slices is required for realizing target dynamics with high fidelity. In particular, adiabatic state preparation requires

* takuya.hatomura@ntt.com

a long operation time for adiabaticity, and thus number of required time slices for adiabatic state preparation is much larger than that for digitization of general time-dependent Hamiltonian dynamics [45]. Suppression of these errors is of great importance for practical usefulness.

In this paper, we propose a decomposition formula which enables us to digitize quantum annealing without digitization errors. We perform numerical simulation and show scaling advantage of our method against the conventional method using Trotterization. We also show that the present method can be applied to quantum annealing with several catalysts. Remarkably, a nonstoquastic catalyst and local counterdiabatic driving are included in applications of the present method.

The present paper is constructed as follows. In Sec. II, we introduce the theory of quantum annealing and digital quantum simulation using Trotterization. We propose our gate-based algorithm of quantum annealing and explain its derivation in Sec. III. We show scaling advantage of our method against the conventional method in Sec. IV. Section V is devoted to discussion. In particular, we discuss application of the present method to quantum annealing with catalyst terms. We give a conclusion in Sec. VI.

II. BACKGROUND

In this section, we give brief summaries of quantum annealing and Trotterization of time-dependent Hamiltonian dynamics.

A. Quantum annealing

Quantum annealing is conducted by using the following Hamiltonian

$$\hat{H}(t) = \lambda(t)\hat{H}_P + (1 - \lambda(t))\hat{V} \quad (1)$$

where \hat{H}_P is the problem Hamiltonian whose ground state is the solution of combinatorial optimization and \hat{V} is the driver Hamiltonian whose ground state can easily be prepared [5, 6]. The solution is obtained by adiabatically changing the time-dependent parameter $\lambda(t)$ from $\lambda(0) = 0$ to $\lambda(T) = 1$ with the annealing time T , which is large enough to satisfy the adiabatic condition [9, 10].

Typically, the problem Hamiltonian is given by the Ising spin glass

$$\hat{H}_P = - \sum_{\substack{i,j=1 \\ (i<j)}}^N J_{ij} \hat{Z}_i \hat{Z}_j - \sum_{i=1}^N h_i \hat{Z}_i, \quad (2)$$

where J_{ij} and h_i are appropriate coupling strength and field strength, respectively. The driver Hamiltonian is

usually given by the transverse-field Hamiltonian

$$\hat{V} = - \sum_{i=1}^N \Gamma_i \hat{X}_i, \quad (3)$$

where Γ_i is field strength. Here, the Pauli matrices of N qubits are expressed as $\{\hat{X}_i, \hat{Y}_i, \hat{Z}_i\}_{i=1}^N$.

B. Digital quantum simulation using Trotterization

We discretize time t as $\{t_m\}_{m=0}^M$, where $0 = t_0 < t_1 < t_2 < \dots < t_M = T$ with an integer M . Then, the unitary time-evolution operator

$$\hat{U}(T, 0) = \mathcal{T} \exp \left(-\frac{i}{\hbar} \int_0^T dt \hat{H}(t) \right), \quad (4)$$

with a time-dependent Hamiltonian $\hat{H}(t)$ and the time-ordering operator \mathcal{T} can be approximated as

$$\begin{aligned} \hat{U}(T, 0) &= \prod_{m=M}^1 \hat{U}(t_m, t_{m-1}) \\ &\approx \prod_{m=M}^1 \hat{U}_d(t_m, t_{m-1}), \end{aligned} \quad (5)$$

where

$$\hat{U}_d(t_m, t_{m-1}) = \exp \left(-\frac{i}{\hbar} \delta t_m \hat{H}(t_m) \right), \quad (6)$$

with $\delta t_m = t_m - t_{m-1}$. The approximation (5) causes discretization errors and it becomes exact if $\delta t_m \rightarrow 0$ for all $m = 1, 2, \dots, M$ as $M \rightarrow \infty$. Note that the argument of the Hamiltonian in Eq. (6) can be any time as long as $t \in [t_{m-1}, t_m]$, but we set it to be $t = t_m$ for simplicity.

Then, we consider Trotterization [40, 41]. Suppose that the Hamiltonian is given by the following form

$$\hat{H}(t) = \sum_{k=1}^K a_k(t) \hat{O}_k, \quad (7)$$

with operators $\{\hat{O}_k\}_{k=1}^K$ and time-dependent coefficients $\{a_k(t)\}_{k=1}^K$. Then, the discretized time-evolution operator (6) can be approximated as

$$\hat{U}_d(t_m, t_{m-1}) \approx \prod_{k=1}^K \hat{U}_k(t_m, t_{m-1}), \quad (8)$$

where

$$\hat{U}_k(t_m, t_{m-1}) = \exp \left(-\frac{i}{\hbar} \delta t_m a_k(t_m) \hat{O}_k \right). \quad (9)$$

Here, we assume that the unitary operator (9) can be implemented on a programmable quantum device as a gate operation. The approximation (8) causes digitization errors and it also becomes exact if $\delta t_m \rightarrow 0$ as $M \rightarrow \infty$.

III. METHOD

Our gate-based quantum algorithm for quantum annealing, which does not cause digitization errors, is as follows:

1. Prepare the ground state of the driver Hamiltonian (3) as the initial state.
2. Repeat the following procedure from $m = 1$ to $m = M$.
 - (a) Apply the ZZ -rotation gate $R_{ZZ}(\delta\Lambda(t_m)J_{ij})$ to all the combinations of the qubits.
 - (b) Apply the z -axis rotation gate $R_Z(\delta\Lambda(t_m)h_i)$ to all the qubits.
 - (c) Apply the x -axis rotation gate $R_X(\delta t_m[1 - \lambda(t_m)]\Gamma_i)$ to all the qubits.
3. Measure the final state with the computational basis $|\sigma\rangle = |\sigma_1, \sigma_2, \dots, \sigma_N\rangle$.

Here, $\delta\Lambda(t_m)$ is given by

$$\delta\Lambda(t_m) = \int_{t_{m-1}}^{t_m} dt \lambda(t), \quad (10)$$

and the computational basis gives $\hat{Z}_i|\sigma_1, \sigma_2, \dots, \sigma_N\rangle = \sigma_i|\sigma_1, \sigma_2, \dots, \sigma_N\rangle$ with $\sigma_i = \pm 1$. Note that the rotation gates are given by

$$\begin{aligned} R_X(\theta_i) &= \exp(i\theta_i\hat{X}_i), & R_Z(\theta_i) &= \exp(i\theta_i\hat{Z}_i) \\ R_{ZZ}(\theta_{ij}) &= \exp(i\theta_{ij}\hat{Z}_i\hat{Z}_j), \end{aligned} \quad (11)$$

with rotation angles θ_i and θ_{ij} . We will show the derivation of the present algorithm below.

A. Decomposition formula

We introduce a decomposition formula utilizing phase degrees of freedom which do not affect measurement outcomes. Suppose that $|\Psi(t)\rangle$ is target dynamics with a Hamiltonian $\hat{H}(t)$ and $\{|\sigma\rangle\}$ is a measurement basis of interest. Another dynamics $|\Psi_f(t)\rangle$ gives the same measurement outcome $|\langle\sigma|\Psi_f(t)\rangle|^2 = |\langle\sigma|\Psi(t)\rangle|^2$ when it is given by

$$|\Psi_f(t)\rangle = \hat{U}_f(t)|\Psi(t)\rangle, \quad (12)$$

where $\hat{U}_f(t)$ is a unitary operator

$$\hat{U}_f(t) = \exp\left(i \sum_{\sigma} f_{\sigma}(t)|\sigma\rangle\langle\sigma|\right), \quad (13)$$

with arbitrary phase $f_{\sigma}(t)$. By inversely solving the Schrödinger equation, we find that the Hamiltonian of the state (12) is given by

$$\hat{H}_f(t) = \hat{U}_f(t)\hat{H}(t)\hat{U}_f^{\dagger}(t) + i\hbar(\partial_t\hat{U}_f(t))\hat{U}_f^{\dagger}(t). \quad (14)$$

We consider digitization of this dynamics (12) with the Hamiltonian (14) instead of the original target dynamics $|\Psi(t)\rangle$ with the Hamiltonian $\hat{H}(t)$ since the measurement outcome is identical. This kind of the idea can also be found in another literature [46, 47].

First, we discretize the time-evolution operator of the state (12) with the Hamiltonian (14) as discussed in Sec. II B. The discretized time-evolution operator (6) is given by

$$\hat{U}_{d,f}(t_m, t_{m-1}) = \exp\left(-\frac{i}{\hbar}\delta t_m\hat{H}_f(t_m)\right). \quad (15)$$

Then, by using a property of unitary transformation, $\exp(\hat{A}) = \hat{U}\exp(\hat{U}^{\dagger}\hat{A}\hat{U})\hat{U}^{\dagger}$, where \hat{A} is an operator and \hat{U} is a unitary operator, we obtain

$$\hat{U}_{d,f}(t_m, t_{m-1}) = \hat{U}_f(t_m)\exp\left(-\frac{i}{\hbar}\delta t_m\hat{H}_f^U(t_m)\right)\hat{U}_f^{\dagger}(t_m), \quad (16)$$

where

$$\begin{aligned} \hat{H}_f^U(t_m) &= \hat{U}_f^{\dagger}(t_m)\hat{H}_f(t_m)\hat{U}_f(t_m) \\ &= \hat{H}(t_m) + i\hbar\hat{U}_f^{\dagger}(t_m)(\partial_t\hat{U}_f(t_m)). \end{aligned} \quad (17)$$

Note that the formula (16) does not cause any error although discretization errors take place to derive the discretized time-evolution operator (15).

B. Application to quantum annealing

Now we discuss application of the decomposition formula (16) to quantum annealing [Eqs. (1 - 3)] with appropriate phase $f_{\sigma}(t)$. Hereafter, we set $\hbar = 1$ according to the conventional notation of quantum annealing.

In quantum annealing, we measure the final state $|\Psi(T)\rangle$ in the computational basis $|\sigma\rangle = |\sigma_1, \sigma_2, \dots, \sigma_N\rangle$. For this measurement basis, we consider the phase $f_{\sigma}(t)$ satisfying

$$\frac{df_{\sigma}(t)}{dt} = -\lambda(t)\left(\sum_{\substack{i,j=1 \\ (i<j)}}^N J_{ij}\sigma_i\sigma_j + \sum_{i=1}^N h_i\sigma_i\right). \quad (18)$$

Then, we find that Eq. (17) is given by

$$\hat{H}_f^U(t_m) = (1 - \lambda(t_m))\hat{V}. \quad (19)$$

Moreover, we obtain

$$\hat{U}_f(t_m) = \exp\left(i\Lambda(t_m)\hat{H}_P\right), \quad (20)$$

with

$$\Lambda(t_m) = \int_0^{t_m} dt \lambda(t). \quad (21)$$

That is, the decomposition formula (16) enables us to divide the discretized time-evolution operator into the unitary operator with the problem Hamiltonian and that with the driver Hamiltonian without any error.

Now we consider the product of the discretized time-evolution operators

$$\prod_{m=M}^1 \hat{U}_{d,f}(t_m, t_{m-1}), \quad (22)$$

which approximately generates the final state of the dynamics $|\Psi_f(T)\rangle$. We notice that the unitary operators $\hat{U}_f(t_m)$ ($m = 1, 2, \dots, M$) between the time slices contribute to this quantity as

$$\hat{U}_f^\dagger(t_m)\hat{U}_f(t_{m-1}) = \exp\left(-i\delta\Lambda(t_m)\hat{H}_P\right), \quad (23)$$

with Eq. (10), the unitary $\hat{U}_f^\dagger(t_1)$ at the right end is given by

$$\hat{U}_f^\dagger(t_1) = \exp\left(-i\delta\Lambda(t_1)\hat{H}_P\right), \quad (24)$$

and the unitary operator $\hat{U}_f(t_M)$ at the left end does not affect the measurement outcome. Therefore, Eq. (22) is equal to

$$\prod_{m=M}^1 \exp\left(-i\delta t_m(1 - \lambda(t_m))\hat{V}\right) \exp\left(-i\delta\Lambda(t_m)\hat{H}_P\right), \quad (25)$$

except for phase factors which do not affect the measurement outcome. To conclude, we derived the proposed algorithm.

IV. NUMERICAL SIMULATION

In this section, we conduct a benchmarking test of our algorithm. The state generated by our algorithm is given by

$$|\Psi_{d,f}(T)\rangle = \prod_{m=M}^1 \left[R_X^{\text{all}}(\delta t_m[1 - \lambda(t_m)]\Gamma_i) \times R_Z^{\text{all}}(\delta\Lambda(t_m)h_i)R_{ZZ}^{\text{all}}(\delta\Lambda(t_m)J_{ij}) \right] |0\rangle, \quad (26)$$

where $|0\rangle$ is the initial state (the ground state of the driver Hamiltonian) and the rotation gates are simplified as

$$R_{X(Z)}^{\text{all}}(\bullet) = \prod_{i=1}^N R_{X(Z)}(\bullet), \quad R_{ZZ}^{\text{all}}(\bullet) = \prod_{\substack{i,j=1 \\ (i<j)}}^N R_{ZZ}(\bullet). \quad (27)$$

As references, we also consider discretized original dynamics

$$|\Psi_d(T)\rangle = \prod_{m=M}^1 \hat{U}_d(t_m, t_{m-1})|0\rangle, \quad (28)$$

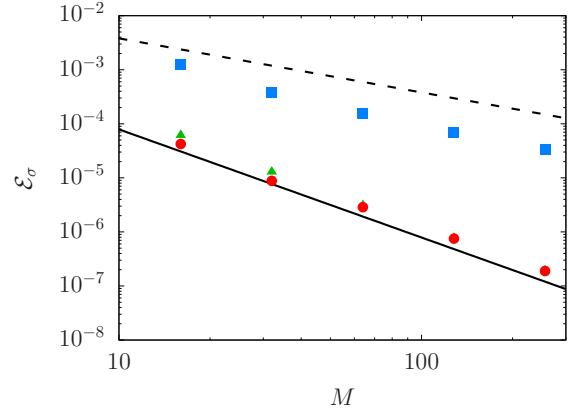


FIG. 1. Errors in digitization of the two-level system. The horizontal axis is the number of time slices M . The red circles represent our algorithm, the green triangles represent the discretized original dynamics, and the blue squares represent the conventional Trotterized dynamics. The black solid line indicates $\mathcal{O}(M^{-2})$ and the black dashed line indicates $\mathcal{O}(M^{-1})$. Here, $h = \Gamma = 1$ and $T = 16$.

and conventional Trotterized dynamics

$$|\Psi_D(T)\rangle = \prod_{m=M}^1 \left[R_X^{\text{all}}(\delta t_m[1 - \lambda(t_m)]\Gamma_i) \times R_Z^{\text{all}}(\delta t_m\lambda(t_m)h_i)R_{ZZ}^{\text{all}}(\delta t_m\lambda(t_m)J_{ij}) \right] |0\rangle. \quad (29)$$

Note that the discretized dynamics (28) cannot directly be realized on gate-based quantum computers.

For evaluating the amount of errors, we consider the following quantity

$$\mathcal{E}_\sigma(|\bullet(T)\rangle) = \left| |\langle\sigma|\Psi(T)\rangle|^2 - |\langle\sigma|\bullet(T)\rangle|^2 \right|, \quad (30)$$

with $\bullet = \Psi_{d,f}, \Psi_d, \Psi_D$. This quantity enables us to evaluate discretization errors in our algorithm because of $|\langle\sigma|\Psi(T)\rangle|^2 = |\langle\sigma|\Psi_f(T)\rangle|^2$, discretization errors in the discretized original dynamics (28), and additional digitization errors in the Trotterized dynamics (29).

In numerical simulation, we assume the linear schedule $\lambda(t) = t/T$ and the uniform time slice $\delta t_m = T/M$ ($m = 1, 2, \dots, M$), and then Eq. (10) is given by $\delta\Lambda(t_m) = (m - 1/2)(T/M^2)$.

First, we consider a two-level system, $J = 0$, $N = 1$, $h_i = h$ ($h > 0$), and $\Gamma_i = \Gamma$ ($\Gamma > 0$). For parameter setting $h = \Gamma = 1$, the annealing time $T = 16$ gives high fidelity to the ground state, $|\langle+1|\Psi(T)\rangle|^2 \approx 0.99988$, and thus the system is adiabatic enough. We plot the errors (30) in the measurement probability of this ground state against the number of time slices in Fig. 1. We find that discretization errors of our algorithm and the original target state behave in a similar way and scale as $\mathcal{O}(M^{-2})$. On the other hand, the Trotterized dynamics with discretization and digitization errors shows worse scaling. This result clearly supports advantage of our algorithm.

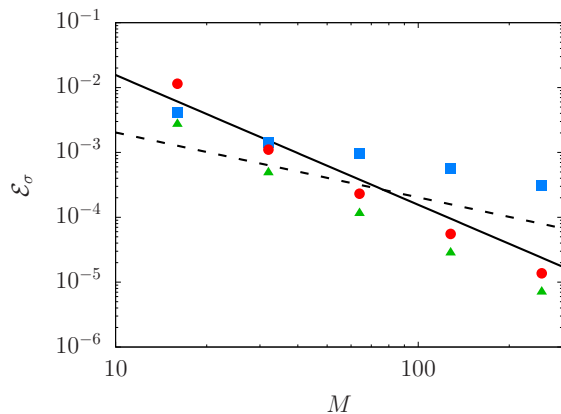


FIG. 2. Errors in digitization of the fully-coupled system with the longitudinal field. The horizontal axis is the number of time slices M . The red circles represent our algorithm, the green triangles represent the discretized original dynamics, and the blue squares represent the conventional Trotterized dynamics. The black solid line indicates $\mathcal{O}(M^{-2})$ and the black dashed line indicates $\mathcal{O}(M^{-1})$. Here, $J = h = \Gamma = 1$, $N = 10$, and $T = 16$.

Next, we consider the following system parameters $J_{ij} = J/N$ ($J > 0$), $h_i = h$ ($h \geq 0$), and $\Gamma_i = \Gamma$ ($\Gamma > 0$). In the case of $h > 0$, the ground state of the problem Hamiltonian is given by $|+1, +1, \dots, +1\rangle$. For parameter setting $J = h = \Gamma = 1$ and $N = 10$, the annealing time $T = 16$ gives high fidelity to the ground state, $|\langle +1, +1, \dots, +1 | \Psi(T) \rangle|^2 \approx 0.99391$, and thus the system is adiabatic enough. We plot the errors (30) in the measurement probability of this ground state against the number of time slices in Fig. 2. We obtain a similar result to the previous example although discretization errors of our algorithm is a little bit larger than discretization errors of the original target dynamics.

Finally, we consider the above example with $h = 0$. In this case, the ground state of the problem Hamiltonian is given by the spin NOON state (a cat state) $|\text{NOON}\rangle = (|+1, +1, \dots, +1\rangle + |-1, -1, \dots, -1\rangle)/\sqrt{2}$. Notably, all the algorithms, i.e., our algorithm, discretized adiabatic driving, digitized adiabatic driving, conserve the parity $\hat{\Pi} = \prod_{i=1}^N \hat{X}_i$, and thus evaluation of the errors (30) in a basis, $|+1, +1, \dots, +1\rangle$ or $|-1, -1, \dots, -1\rangle$, is enough to discuss errors (30) in the measurement probability of this ground state (see, e.g., Ref. [48]). Therefore, we again consider the basis $|+1, +1, \dots, +1\rangle$. For parameter setting $J = \Gamma = 1$ and $N = 10$, the annealing time $T = 64$ gives fidelity to the all-up state, $|\langle +1, +1, \dots, +1 | \Psi(T) \rangle|^2 \approx 0.49891$, which corresponds to the fidelity to the ground state, $|\langle \text{NOON} | \Psi(T) \rangle|^2 \approx 0.99782$, and thus the system is adiabatic enough. We plot the errors (30) in the measurement probability of the all-up state $|+1, +1, \dots, +1\rangle$ against the number of time slices in Fig. 3. We find that our algorithm causes larger discretization errors than the original target dynamics, but it has similar scaling $\mathcal{O}(M^{-2})$ which

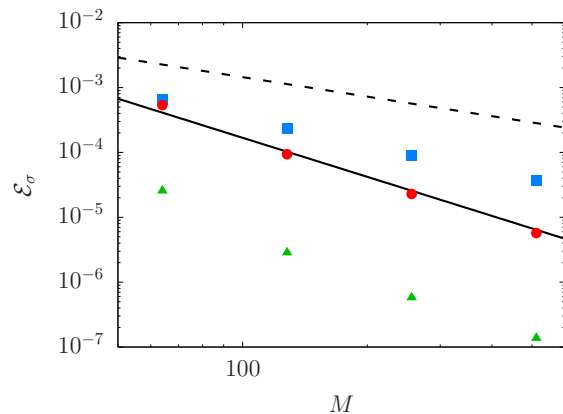


FIG. 3. Errors in digitization of the fully-coupled system without the longitudinal field. The horizontal axis is the number of time slices M . The red circles represent our algorithm, the green triangles represent the discretized original dynamics, and the blue squares represent the conventional Trotterized dynamics. The black solid line indicates $\mathcal{O}(M^{-2})$ and the black dashed line indicates $\mathcal{O}(M^{-1})$. Here, $J = \Gamma = 1$, $h = 0$, $N = 10$, and $T = 64$.

is clearly better than the conventional Trotterization.

V. DISCUSSION

A. Behavior of errors

Our algorithm causes larger discretization errors than discretization of the original target dynamics when we consider many-body systems. This may be based on the fact that our Hamiltonian (14) has various many-body and nonlocal interactions, which are generated by $\hat{U}_f(t)\hat{H}(t)\hat{U}_f^\dagger(t)$, while the original Hamiltonian $\hat{H}(t)$ consists of 2-local interactions at most.

Scaling behavior of discretization and digitization errors is also of interest. A conventional analysis on discretization and digitization errors predicts $\mathcal{O}(\delta t_m^2)$ errors for each time slice and $\mathcal{O}(\delta t_m^2 \times M) = \mathcal{O}(T^2/M)$ errors for total M time slices [40, 41]. Surprisingly, we found that scaling of discretization errors is rather close to $\mathcal{O}(M^{-2})$, while scaling of digitization errors seems $\mathcal{O}(M^{-1})$. Here, we plot infidelity of discretized dynamics and digitized dynamics to the target dynamics, $\mathcal{I}_m(|\bullet(t_m)\rangle) = 1 - |\langle \Psi(t_m) | \bullet(t_m) \rangle|^2$, where $\bullet = \Psi_d, \Psi_D$, in Fig. 4 by using the two-level systems with the above parameter setting. We notice that deviations from target dynamics are not uniform, that is, the total amount of errors is not $\mathcal{O}(\delta t_m^2 \times M)$ but $\mathcal{O}(\sum_{m=1}^M p_m \delta t_m^2)$ with certain weight p_m . Difference in weight causes scaling advantage of our algorithm against the conventional Trotterization. Note that scaling of errors in our algorithm and discretized dynamics may be $\mathcal{O}(\sum_{m=1}^M p_m \delta t_m^2) = \mathcal{O}(aM^{-1} + bM^{-2})$ with $a \ll b$, but scaling of $\mathcal{O}(M^{-1})$

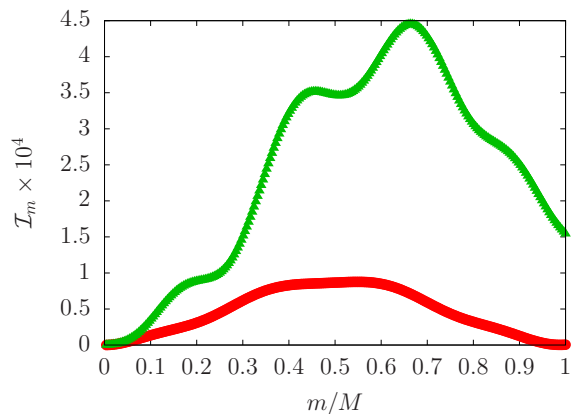


FIG. 4. Infidelity of discretized dynamics and digitized dynamics to the target dynamics. The horizontal axis is the normalized time step m/M with $M = 256$. The red circles represent infidelity of discretized dynamics and the green triangles represent that of digitized dynamics. Here, $J = 0$, $N = 1$, $h = \Gamma = 1$, and $T = 16$.

does not appear in the parameter range we studied, in which discretization errors are significantly suppressed.

B. Other applications

We discussed elimination of digitization errors and its effects on discretization errors. It is also of great importance to suppress adiabatic errors in target dynamics for reducing the annealing time. Introduction of catalyst terms is one of the ways of improving adiabaticity [11–14]. A Hamiltonian of quantum annealing with catalysts is typically given by

$$\hat{H}(t) = \lambda(t)\hat{H}_P + \lambda(t)(1 - \lambda(t))\hat{H}_C + (1 - \lambda(t))\hat{V}, \quad (31)$$

where \hat{H}_C is the catalyst Hamiltonian. The XX -interaction catalyst $\hat{H}_{XX} = \sum_{i,j=1}^N (i < j) K_{ij} \hat{X}_i \hat{X}_j$ with positive K_{ij} is known as a nonstoquastic catalyst and it has ability to remove the first-order transitions in some models [11, 12]. The Z -field catalyst $\hat{H}_Z = \sum_{i=1}^N \tilde{h}_i \hat{Z}_i$ was also introduced as bias fields and it can also improve adiabaticity when the sign of the bias fields are appropriate [13, 14].

In counterdiabatic driving, for a given Hamiltonian $\hat{H}(t) = \sum_n E_n(t) |n(t)\rangle \langle n(t)|$, where $E_n(t)$ is an energy eigenvalue and $|n(t)\rangle$ is the corresponding energy eigenstate, we introduce the counterdiabatic Hamiltonian

$$\hat{H}_{CD}(t) = i\hbar \sum_{\substack{m,n \\ m \neq n}} |m(t)\rangle \langle m(t)| \partial_t n(t) \langle n(t)|, \quad (32)$$

which enables us to completely eliminate adiabatic errors [18–20]. However, its construction requires an exponential computational cost. Local counterdiabatic driving has been paid attention as a means of suppressing

some nonadiabatic transitions in a practical way (see, Refs. [15–17] and references therein). For the quantum annealing Hamiltonian (1 - 3), the simplest way of local counterdiabatic driving is application of a local Y -field, $\hat{H}_{LCD}(t) = \sum_{i=1}^N \alpha(t) \hat{Y}_i$. The time-dependent coefficient $\alpha(t)$ can be determined in various ways, e.g., the variational (algebraic) approach [21, 22] or the mean-field (classical) approach [26, 27]. Local counterdiabatic driving can be regarded as introduction of a well-designed Y -field catalyst.

Application of our algorithm to quantum annealing with these catalysts enables us to divide the discretized time-evolution operator into a unitary operator with Z terms (the problem Hamiltonian and the Z -field catalyst) and a unitary operator with the others (the driver Hamiltonian, the XX -interaction catalyst, the Y -field catalyst). Except for the case where the XX -interaction catalyst and the Y -field catalyst coexist, these unitary operators can be divided into ZZ -rotation gate, z -axis rotation gate, XX -rotation gate, and x -axis rotation gate without digitization errors. Note that implementation of single-spin rotation in a tilted axis is required when the Y -field catalyst is applied. We can realize this gate operation by using the z -axis rotation gate and the x -axis rotation gate as $R_Z(-\psi/2)R_X(\phi)R_Z(\psi/2) = R_{X \cos \psi + Y \sin \psi}(\phi)$ with a tilt angle ψ and a rotation angle ϕ . Remarkably, as a result of the commutability between ZZ interactions and Z fields, the above rotation gates can just be regarded as modulation of the x -axis rotation gate and the z -axis rotation gate in our algorithm. In conclusion, we can realize gate-based quantum annealing enhanced by the various catalysts without digitization errors.

In this paper, we focused on the Ising spin glass as the problem Hamiltonian, but our method can be extended to problems including higher-order interactions such as $\hat{Z}_i \hat{Z}_j \hat{Z}_k$ by adding $\sigma_i \sigma_j \sigma_k$ in Eq. (18) although it requires the ZZZ rotation gate. Since our decomposition formula is quite general, application of our decomposition formula to other quantum information processing or other types of Hamiltonians is also of great interest. We leave further study as the future work.

VI. CONCLUSION

We proposed the gate-based algorithm for quantum annealing which does not cause digitization errors. It was shown that our algorithm has clear scaling advantage against the conventional Trotterization approach. We also showed that the present method can be applied to quantum annealing with the combinations of the nonstoquastic XX -interaction, the bias Z -field, and the counterdiabatic Y -field catalysts except for the coexistence of the XX -interaction and the Y -field catalysts. We believe that our proposal paves the way for realization of high-fidelity time-dependent Hamiltonian simulation including digital implementation of enhanced quantum annealing.

ACKNOWLEDGMENTS

This work was supported by JST Moonshot R&D Grant Number JPMJMS2061.

-
- [1] B. Korte and J. Vygen, *Combinatorial optimization: Theory and algorithms*, 6th ed. (Springer Berlin, Heidelberg, 2018).
- [2] F. Neukart, G. Compostella, C. Seidel, D. von Dollen, S. Yarkoni, and B. Parney, Traffic flow optimization using a quantum annealer, *Frontiers in ICT* **4**, 301656 (2017).
- [3] E. G. Rieffel, D. Venturelli, B. O’Gorman, M. B. Do, E. M. Prystay, and V. N. Smelyanskiy, A case study in programming a quantum annealer for hard operational planning problems, *Quantum Information Processing* **14**, 1 (2015).
- [4] G. Rosenberg, P. Haghnegahdar, P. Goddard, P. Carr, K. Wu, and M. L. D. Prado, Solving the optimal trading trajectory problem using a quantum annealer, *IEEE Journal on Selected Topics in Signal Processing* **10**, 1053 (2016).
- [5] T. Kadowaki and H. Nishimori, Quantum annealing in the transverse ising model, *Physical Review E* **58**, 5355 (1998).
- [6] E. Farhi, J. Goldstone, S. Gutmann, and M. Sipser, Quantum computation by adiabatic evolution, [arXiv:quant-ph/0001106](https://arxiv.org/abs/quant-ph/0001106) (2000).
- [7] P. Hauke, H. G. Katzgraber, W. Lechner, H. Nishimori, and W. D. Oliver, Perspectives of quantum annealing: methods and implementations, *Reports on Progress in Physics* **83**, 054401 (2020).
- [8] A. Lucas, Ising formulations of many np problems, *Frontiers in Physics* **2**, 5 (2014).
- [9] T. Kato, On the adiabatic theorem of quantum mechanics, *Journal of the Physical Society of Japan* **5**, 435 (1950).
- [10] S. Jansen, M.-B. Ruskai, and R. Seiler, Bounds for the adiabatic approximation with applications to quantum computation, *Journal of Mathematical Physics* **48**, 102111 (2007).
- [11] Y. Seki and H. Nishimori, Quantum annealing with anti-ferromagnetic fluctuations, *Physical Review E* **85**, 051112 (2012).
- [12] T. Albash, Role of nonstoquastic catalysts in quantum adiabatic optimization, *Physical Review A* **99**, 042334 (2019).
- [13] T. Graß, Quantum annealing with longitudinal bias fields, *Physical Review Letters* **123**, 120501 (2019).
- [14] T. Albash and M. Kowalsky, Diagonal catalysts in quantum adiabatic optimization, *Physical Review A* **103**, 022608 (2021).
- [15] E. Torrontegui, S. Ibáñez, S. Martínez-Garaot, M. Modugno, A. del Campo, D. Guéry-Odelin, A. Ruschhaupt, X. Chen, and J. G. Muga, Shortcuts to adiabaticity, *Advances In Atomic, Molecular, and Optical Physics* **62**, 117 (2013).
- [16] D. Guéry-Odelin, A. Ruschhaupt, A. Kiely, E. Torrontegui, S. Martínez-Garaot, and J. G. Muga, Shortcuts to adiabaticity: Concepts, methods, and applications, *Reviews of Modern Physics* **91**, 045001 (2019).
- [17] T. Hatomura, Shortcuts to adiabaticity: theoretical framework, relations between different methods, and versatile approximations, *Journal of Physics B: Atomic, Molecular and Optical Physics* **57**, 102001 (2024).
- [18] M. Demirplak and S. A. Rice, Adiabatic population transfer with control fields, *The Journal of Physical Chemistry A* **107**, 9937 (2003).
- [19] M. Demirplak and S. A. Rice, On the consistency, extremal, and global properties of counterdiabatic fields, *The Journal of Chemical Physics* **129**, 154111 (2008).
- [20] M. V. Berry, Transitionless quantum driving, *Journal of Physics A: Mathematical and Theoretical* **42**, 365303 (2009).
- [21] D. Sels and A. Polkovnikov, Minimizing irreversible losses in quantum systems by local counterdiabatic driving., *Proceedings of the National Academy of Sciences of the United States of America* **114**, E3909 (2017).
- [22] T. Hatomura and K. Takahashi, Controlling and exploring quantum systems by algebraic expression of adiabatic gauge potential, *Physical Review A* **103**, 012220 (2021).
- [23] K. Takahashi and A. del Campo, Shortcuts to adiabaticity in krylov space, *Physical Review X* **14**, 011032 (2024).
- [24] B. Bhattacharjee, A lanczos approach to the adiabatic gauge potential, [arXiv:2302.07228](https://arxiv.org/abs/2302.07228) (2023).
- [25] P. W. Claeys, M. Pandey, D. Sels, and A. Polkovnikov, Floquet-engineering counterdiabatic protocols in quantum many-body systems, *Physical Review Letters* **123**, 090602 (2019).
- [26] T. Hatomura, Shortcuts to adiabaticity in the infinite-range ising model by mean-field counter-diabatic driving, *Journal of the Physical Society of Japan* **86**, 094002 (2017).
- [27] T. Hatomura and T. Mori, Shortcuts to adiabatic classical spin dynamics mimicking quantum annealing, *Physical Review E* **98**, 032136 (2018).
- [28] A. D. King, J. Carrasquilla, J. Raymond, I. Ozfidan, E. Andriyash, A. Berkley, M. Reis, T. Lanting, R. Harris, F. Altomare, K. Boothby, P. I. Bunyk, C. Enderud, A. Fréchet, E. Hoskinson, N. Ladizinsky, T. Oh, G. Poulin-Lamarre, C. Rich, Y. Sato, A. Y. Smirnov, L. J. Swenson, M. H. Volkmann, J. Whittaker, J. Yao, E. Ladizinsky, M. W. Johnson, J. Hilton, and M. H. Amin, Observation of topological phenomena in a programmable lattice of 1,800 qubits, *Nature* **560**, 456 (2018).
- [29] A. D. King, S. Suzuki, J. Raymond, A. Zucca, T. Lanting, F. Altomare, A. J. Berkley, S. Ejtemaee, E. Hoskinson, S. Huang, E. Ladizinsky, A. J. R. MacDonald, G. Marsden, T. Oh, G. Poulin-Lamarre, M. Reis, C. Rich, Y. Sato, J. D. Whittaker, J. Yao, R. Harris, D. A. Lidar, H. Nishimori, and M. H. Amin, Coherent quantum annealing in a programmable 2,000 qubit ising chain, *Nature Physics* **18**, 1324 (2022).
- [30] A. D. King, J. Raymond, T. Lanting, R. Harris, A. Zucca, F. Altomare, A. J. Berkley, K. Boothby, S. Ejtemaee,

- C. Enderud, E. Hoskinson, S. Huang, E. Ladizinsky, A. J. R. MacDonald, G. Marsden, R. Molavi, T. Oh, G. Poulin-Lamarre, M. Reis, C. Rich, Y. Sato, N. Tsai, M. Volkmann, J. D. Whittaker, J. Yao, A. W. Sandvik, and M. H. Amin, Quantum critical dynamics in a 5,000-qubit programmable spin glass, *Nature* **617**, 61 (2023).
- [31] F. Arute, K. Arya, R. Babbush, D. Bacon, J. C. Bardin, R. Barends, R. Biswas, S. Boixo, F. G. Brandao, D. A. Buell, B. Burkett, Y. Chen, Z. Chen, B. Chiaro, R. Collins, W. Courtney, A. Dunsworth, E. Farhi, B. Foxen, A. Fowler, C. Gidney, M. Giustina, R. Graff, K. Guerin, S. Habegger, M. P. Harrigan, M. J. Hartmann, A. Ho, M. Hoffmann, T. Huang, T. S. Humble, S. V. Isakov, E. Jeffrey, Z. Jiang, D. Kafri, K. Kechedzhi, J. Kelly, P. V. Klimov, S. Knysh, A. Korotkov, F. Kostritsa, D. Landhuis, M. Lindmark, E. Lucero, D. Lyakh, S. Mandrà, J. R. McClean, M. McEwen, A. Megrant, X. Mi, K. Michielsen, M. Mohseni, J. Mutus, O. Naaman, M. Neeley, C. Neill, M. Y. Niu, E. Ostby, A. Petukhov, J. C. Platt, C. Quintana, E. G. Rieffel, P. Roushan, N. C. Rubin, D. Sank, K. J. Satzinger, V. Smelyanskiy, K. J. Sung, M. D. Trevithick, A. Vainsencher, B. Villalonga, T. White, Z. J. Yao, P. Yeh, A. Zalcman, H. Neven, and J. M. Martinis, Quantum supremacy using a programmable superconducting processor, *Nature* **574**, 505 (2019).
- [32] Y. Wu, W.-S. Bao, S. Cao, F. Chen, M.-C. Chen, X. Chen, T.-H. Chung, H. Deng, Y. Du, D. Fan, M. Gong, C. Guo, C. Guo, S. Guo, L. Han, L. Hong, H.-L. Huang, Y.-H. Huo, L. Li, N. Li, S. Li, Y. Li, F. Liang, C. Lin, J. Lin, H. Qian, D. Qiao, H. Rong, H. Su, L. Sun, L. Wang, S. Wang, D. Wu, Y. Xu, K. Yan, W. Yang, Y. Yang, Y. Ye, J. Yin, C. Ying, J. Yu, C. Zha, C. Zhang, H. Zhang, K. Zhang, Y. Zhang, H. Zhao, Y. Zhao, L. Zhou, Q. Zhu, C.-Y. Lu, C.-Z. Peng, X. Zhu, and J.-W. Pan, Strong quantum computational advantage using a superconducting quantum processor, *Physical Review Letters* **127**, 180501 (2021).
- [33] D. Bluvstein, S. J. Evered, A. A. Geim, S. H. Li, H. Zhou, T. Manovitz, S. Ebadi, M. Cain, M. Kalinowski, D. Hangleiter, J. Pablo, B. Ataiades, N. Maskara, I. Cong, X. Gao, P. S. Rodriguez, T. Karolyshyn, G. Semeghini, M. J. Gullans, M. Greiner, V. Vuletić, and M. D. Lukin, Logical quantum processor based on reconfigurable atom arrays, *Nature* **626**, 58 (2024).
- [34] M. Steffen, W. van Dam, T. Hogg, G. Breyta, and I. Chuang, Experimental implementation of an adiabatic quantum optimization algorithm, *Physical Review Letters* **90**, 067903 (2003).
- [35] R. Barends, A. Shabani, L. Lamata, J. Kelly, A. Mezzacapo, U. L. Heras, R. Babbush, A. G. Fowler, B. Campbell, Y. Chen, Z. Chen, B. Chiaro, A. Dunsworth, E. Jeffrey, E. Lucero, A. Megrant, J. Y. Mutus, M. Neeley, C. Neill, P. J. J. O'Malley, C. Quintana, P. Roushan, D. Sank, A. Vainsencher, J. Wenner, T. C. White, E. Solano, H. Neven, and J. M. Martinis, Digitized adiabatic quantum computing with a superconducting circuit, *Nature* **534**, 222 (2016).
- [36] N. N. Hegade, K. Paul, Y. Ding, M. Sanz, F. Albarrán-Arriagada, E. Solano, and X. Chen, Shortcuts to adiabaticity in digitized adiabatic quantum computing, *Physical Review Applied* **15**, 024038 (2021).
- [37] N. N. Hegade, X. Chen, and E. Solano, Digitized counterdiabatic quantum optimization, *Physical Review Research* **4**, L042030 (2022).
- [38] D. van Vreumingen, Gate-based counterdiabatic driving with complexity guarantees, *arXiv:2406.08064* (2024).
- [39] T. Hatomura, Benchmarking adiabatic transformation by alternating unitaries, *arXiv:2407.12326* (2024).
- [40] J. Huyghebaert and H. D. Raedt, Product formula methods for time-dependent schrodinger problems, *Journal of Physics A: Mathematical and General* **23**, 5777 (1990).
- [41] S. Lloyd, Universal quantum simulators, *Science* **273**, 1073 (1996).
- [42] L. K. Kovalsky, F. A. Calderon-Vargas, M. D. Grace, A. B. Magann, J. B. Larsen, A. D. Baczewski, and M. Sarovar, Self-healing of trotter error in digital adiabatic state preparation, *Physical Review Letters* **131**, 060602 (2023).
- [43] T. Hatomura, State-dependent error bound for digital quantum simulation of driven systems, *Physical Review A* **105**, L050601 (2022).
- [44] T. Hatomura, Scaling of errors in digitized counterdiabatic driving, *New Journal of Physics* **25**, 103025 (2023).
- [45] G. B. Mbeng, L. Arceci, and G. E. Santoro, Optimal working point in digitized quantum annealing, *Physical Review B* **100**, 224201 (2019).
- [46] T. Hatomura, Time rescaling of nonadiabatic transitions, *SciPost Physics* **15**, 036 (2023).
- [47] T. Hatomura, Energy-saving fast-forward scaling, *arXiv:2402.10683* (2024).
- [48] T. Hatomura, A. Yoshinaga, Y. Matsuzaki, and M. Tatsu, Quantum metrology based on symmetry-protected adiabatic transformation: imperfection, finite time duration, and dephasing, *New Journal of Physics* **24**, 033005 (2022).